

WAVE TANK STUDIES ON CHEMICAL DISPERSANT EFFECTIVENESS: DISPERSED OIL DROPLET SIZE DISTRIBUTION

Z. LI[†], K. LEE, P. KEPKAY, T. KING & W. YEUNG
*Center for Offshore Oil and Gas Environmental
Research, Fisheries and Oceans, Canada, Dartmouth,
Nova Scotia, B2Y 4A2, Canada*

M.C. BOUFADEL
*Department of Civil and Environmental Engineering,
Temple University, Philadelphia, Pennsylvania, 19122,
USA*

A.D. VENOSA
*National Risk Management Research Lab, U.S. EPA,
Cincinnati, OH 45268, USA*

Abstract. In evaluation of chemical dispersant effectiveness, the two most important factors that need to be addressed and fully characterized in terms of efficacy are energy dissipation rate and particle size distribution. A wave tank facility was designed and constructed to specifically address these factors in controlled oil dispersion studies. The particle size distribution of the dispersed oil was quantified by a laser *in-situ* scattering and transmissometer (LISST-100X). The size distribution and morphology of the dispersed oil were characterized by an image analysis system based on a microscope fitted with transmitted light and ultraviolet-epifluorescence illumination. Time-series particle size distribution during physical and chemical dispersion of crude oil under a variety of non-breaking and breaking waves are presented.

Keywords: wave tank, dispersant, oil droplet, LISST, waves

[†] To whom correspondence should be addressed. E-mail: LiZ@mar.dfo-mpo.gc.ca

1. Introduction

The application of chemical dispersants is considered to be one of the primary oil spill countermeasures for reducing the overall environmental impact of marine oil spills (NRCNA, 2005; NRC, 2005; Lessard and Demarco, 2000). In addition to operational convenience, application of dispersants to treat oil slicks on the sea surface has advantages to minimize the harmful effect of floating oil on animals such as birds and marine mammals that frequent the water surface, and to reduce the risk of oil slicks contaminating coastal and/or shore-line environments.

Dispersants are chemicals that contain surfactants that reduce the surface tension between oil and water, resulting in the formation of oil droplets (oil-in-water emulsion). The dispersion of oil slicks is significantly enhanced in the presence of waves. Waves provide mixing energy, which breaks the surface oil film and propels oil droplets into the water column. Thus, in the context of oil spill response operations, dispersion is a physical-chemical process, whose effectiveness depends on the chemical properties of both dispersant and the oil and the mixing energy generated by the physical action of waves (NRC, 2005; Fingas, 2000). The hydrodynamic behaviour may dramatically influence natural and chemical dispersion of oil (Shaw, 2003; Delvigne and Sweeney, 1988). In particular, breaking waves play a crucial role in the mixing of oil and dispersant and hence the dispersion of an oil slick (Shaw, 2003). Breaking of waves occurs when the forward horizontal velocity of water in a wave crest is greater than the wave propagation speed. These waves cause velocity shear and hence result in the mixing of oil and dispersant. In turbulent flows, the velocity shear results from both spatial and temporal (turbulent) variation of velocities, but usually the turbulence contribution is dominant. Velocity shear with its associated friction also causes the dissipation of kinetic energy of the fluid. Of interest is the kinetic energy dissipation rate per unit mass, ε , which varies both in time and space. One may use velocity measurements in a selected water body to compute the shear, and subsequently the energy dissipation rate.

The effectiveness of a particular dispersant is typically evaluated at various scales ranging from the smallest (10 cm, typical of the Swirling Flask Test in the laboratory) to the largest (10s to 100s m, typical of

field scale open water dispersion tests). In terms of product selection for spill response operations, standard laboratory assays for the evaluation of oil dispersant effectiveness such as the swirling flask test have limitations due to insufficient mixing energy and/or failure to account for the transport and interaction between oil and dispersant in water column (Sorral, 2004a, b; Venosa *et al.*, 2003). Testing at sea, however, is expensive and not always reproducible due to uncontrolled environmental variables, and hence unrealistic for routine testing of different dispersants on different oils. To address these concerns, a wave tank facility was constructed for evaluation of chemical oil dispersant effectiveness at intermediate or pilot scales.

The current hypothesis is that the energy dissipation rate per unit mass, ϵ , plays a major role in the effectiveness of a dispersant. Conservation of ϵ between the wave tank and actual field conditions provides support for the use of our test system to evaluate the operational effectiveness of chemical oil dispersants. Preliminary hydrodynamic tests have demonstrated that the non-breaking waves and breaking waves that were generated in our test tank facility were similar to the reported energy dissipation rates for natural waters (Venosa *et al.*, 2005; Delvigne, 1988).

2. Materials and Methods

2.1. WAVE TANK FACILITIES

Figure 1 presents the schematic of the wave tank. The tank facility measures 32 m long, 0.6 m wide, and 2 m high. The water depth during the present experiments was 1.50 m. Different waves can be generated by a paddle situated at one end of the tank linked to an adjustable cam that controls its stroke length to alter wave-height characteristics. The wave frequency (and subsequently wave length) is controlled by the rotation speed of the cam. The computer-controlled wave-generator is capable of producing both regular non-breaking waves and breaking waves with designated length, height and frequency. The system is very useful for dispersion studies because recurrent breaking of waves can be generated at the same location. This is done by superimposing a wave of one frequency onto a wave of another frequency, causing the wave to break under different inertial forces. Calibration of non-breaking

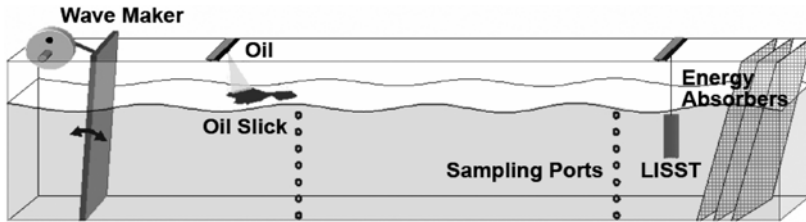


Figure 1. Schematic representation of the wave tank.

and breaking-wave energy was conducted using a scalable parameter, energy dissipation rate. The details of wave energy calibration have been reported elsewhere (Venosa *et al.*, 2005).

2.2. EXPERIMENTAL PROCEDURES

The wave tank study on chemical dispersant effectiveness testing was conducted using two crude oils (MESA and Alaska North Slope (ANS) oil), three dispersants (water, Corexit 9500 and SPC1000), and three wave energy conditions (a regular wave, a spilling breaking wave, and a plunging breaking wave).

A three-factor mixed-level factorial experiment was designed. The three factors and their levels are: two oils, three dispersants, and three waves. Hence, 18 treatments were set up for this dispersant effectiveness study experiment; with triplicate runs for each treatment, resulting in 54 runs for the entire experiment. Different treatments were conducted in a random order to minimize the impacts of other confounding factors such as temperature, salinity, and wind on the dispersant effectiveness of crude oil.

2.3. TOTAL PETROLEUM HYDROCARBONS

The dispersed oil in aqueous samples was extracted with dichloromethane and measured with a DU series 60 ultraviolet-visible spectrophotometer (Beckman Instruments, Inc., Fullerton, CA) capable of measuring absorbance at 340, 370, and 400 nm (Venosa *et al.*, 2002). These absorbance values were used because they represent different locations within the absorbance curve. A 10 mm cuvette with 1 cm path length was used for measurement and dichloromethane was used as the reference blank. For all analyses the cuvette was used with a polytetrafluoroethylene cover.

The direct ultraviolet fluorescence spectroscopy was also applied to monitor the dispersed/dissolved oil in seawater using a method reported previously (Kepkay *et al.*, 2002). Briefly, samples collected from the wave tank at specified times and locations were vigorously shaken by hand, and 3 mL of the suspension was rapidly transferred to an ultraviolet-grade methyl acrylate disposable cuvette (VWR International Inc., Mississauga, ON). The suspension was immediately scanned in the dissolved/dispersed fraction using a QM-1 spectrofluorometer running FeliX software (PTI, Inc., Birmingham, NJ). The optimal excitation wavelength that produced the highest emission peaks was 320 nm. This wavelength with a slit width of ± 2 nm was used in all subsequent emission scans from 340 to 500 nm.

2.4. PARTICLE SIZE DISTRIBUTION

Oil droplet size distribution inside the wave tank was determined by a Type C LISST-100X particle counter (Sequoia, Seattle, WA), which has 32 particle size intervals logarithmically spaced from 2.5 to 500 μ m in diameter, with the upper size in each bin 1.18 times the lower. Particle size distribution is expressed as the average volumetric concentration of oil droplets falling into each interval of the size range. In general, the particle size distribution measured using LISST fits a log-normal distribution, which has been extensively used for measuring aerosol size distribution in natural environment (Hinds, 1999). The data acquisition is conducted at real time operation mode throughout each experimental run, with an average of ten measurements for each sample being taken every 3 s. The *in-situ* dispersed oil droplet size distribution and total oil concentration are measured at one horizontal location (16 m downstream of the flap) and three different depths (30, 75, and 120 cm under water) over eight continual time periods.

3. Results and Discussion

3.1. HYDRODYNAMICS OF THE WAVE TANK

Three different wave conditions were selected to represent the typical wave energy conditions at sea. Photos of the three wave conditions are

presented in Figure 2. The three wave types are: (1) regularly non-breaking waves; (2) spilling breakers; and (3) plunging breakers.

Regular non-breaking and breaking wave profiles were recorded using wave gauges that were deployed at different locations of the wave tank. For the regular non-breaking waves, uniform waves were produced throughout the entire length of the wave tank, including the initial wave generation zone, intermediate wave propagation zone, and the end of the wave tank nearest to the wave absorbers. The observed wave height (0.17 m) matches well with the theoretical prediction based on linear theory of waves (0.16 m). The constant wave heights throughout the tank suggest that the energy dissipation rate of the regular waves was small. Most of the wave energy was absorbed when wave were propagated to the end of the tank by the wave absorbers. The smooth wave profiles recorded by the wave gauge near the end of the wave tank indicates the reflection of the tail end of the tank was effectively controlled through the proper functioning of the wave absorbers.

Breaking waves were generated by superposition of two different waves. The high frequency with high wave height (0.17 m) followed by low frequency with low wave height (0.11 m), is clearly shown with the wave profile obtained at 2 m from the wave generation flap. Superposition of the waves occurred immediately prior to the breaking zone, creating a transitional wave height as much as 0.28 m, which is equal to the sum of the two component waves. The instant breaking waves and dissipation of wave energy in the mixing zone were captured by the wave gauges that are deployed in the breaking zone and the one further down stream of the wave tank. The post breaker wave height was reduced to 0–0.03 m, indicating that most of the wave energy was dissipated from the surface water body to the bulk water body as micro-scale turbulence.

Similar wave profiles were obtained for the spilling breaking waves, one with a stroke of 6 cm and the other with a stroke of 7 cm. The observed maximum wave height (after superposition of the two components) was 0.21 and 0.25 m, respectively, for $S = 6$ and 7 cm conditions. Breaking waves occurred at approximately the same location as the plunging breaker. The spilling breakers, especially for $S = 6$ cm, were less violent than the plunging breaker. Since wave energies are proportional to the square of wave height, spilling breakers are likely to have low energy dissipation rates compared to plunging

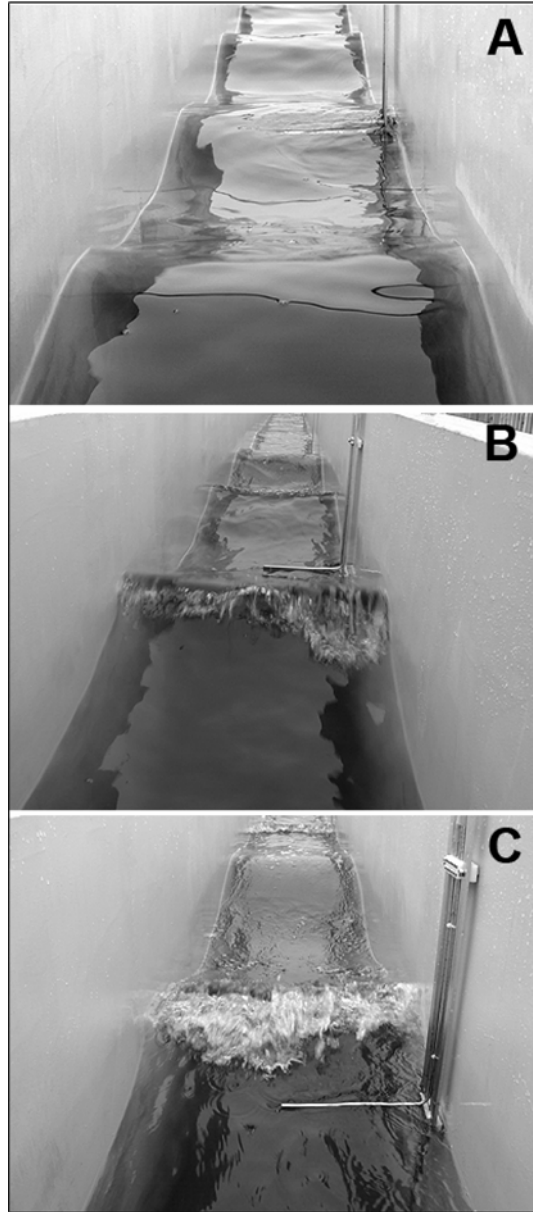


Figure 2. Photographs of three representative wave conditions: (A) regular non-breaking wave, (B) spilling breaking wave, and (C) plunging breaking wave.

breaking waves, assuming the time scale of these breakers are similar. Given our goal is to find a variety of representative wave conditions of the real sea states, the spilling breaker with a stroke of 7 cm was selected along with the plunging breaker and the regular non-breaking wave for the next chemical dispersant effectiveness test.

3.2. DISPERSANT EFFECTIVENESS STUDY

A preliminary dispersant effectiveness study was conducted in the wave tank under three wave conditions. Dispersant effectiveness was evaluated by monitoring oil distribution using the LISST-100X and ultra-violet fluoremeter (UVF).

Figure 3 shows the total dispersed oil concentration at three different depths, namely near the surface, in the middle, and near the bottom, as recorded by LISST-100X. Oil concentrations at the surface and in the middle of the tank are similar, but they appear to be more dynamic at the bottom. The fluctuation of dispersed oil concentration with time was pronounced during the first hour under a breaking wave regime. After the paddle was stopped to maintain the tank in a quiescent state, oil concentrations were less variable for all three depths. The total oil concentrations slightly increased over time, indicating that resurfacing of the dispersed oil was effective at quiescent conditions. The total oil concentration distribution in the wave tank over time was consistent with the dispersed oil droplet size distribution.

Figure 4 shows the mass mean diameter (MMD) of the dispersed oil droplet size distribution at three different depths in the water column. At near surface and in the middle of the tank water, oil droplets were usually less than 100 μm , whereas at near bottom, MMD of the dispersed oil droplets were more than 200 μm within the first hour and declined to less than 100 μm after 2 h dispersion. The MMD of the dispersed oil droplets remained constant throughout the last 2 h during the quiescent hydrodynamic regime, indicating that although resurfacing the submerged oil droplets is inevitable, recoalescence of the small dispersed oil droplets into large oil droplets may not necessarily occur because of the presence residual surfactant from the chemical dispersant.

Total oil concentration and dispersed oil droplet size distribution data were also obtained for the regular wave and the spilling breaking

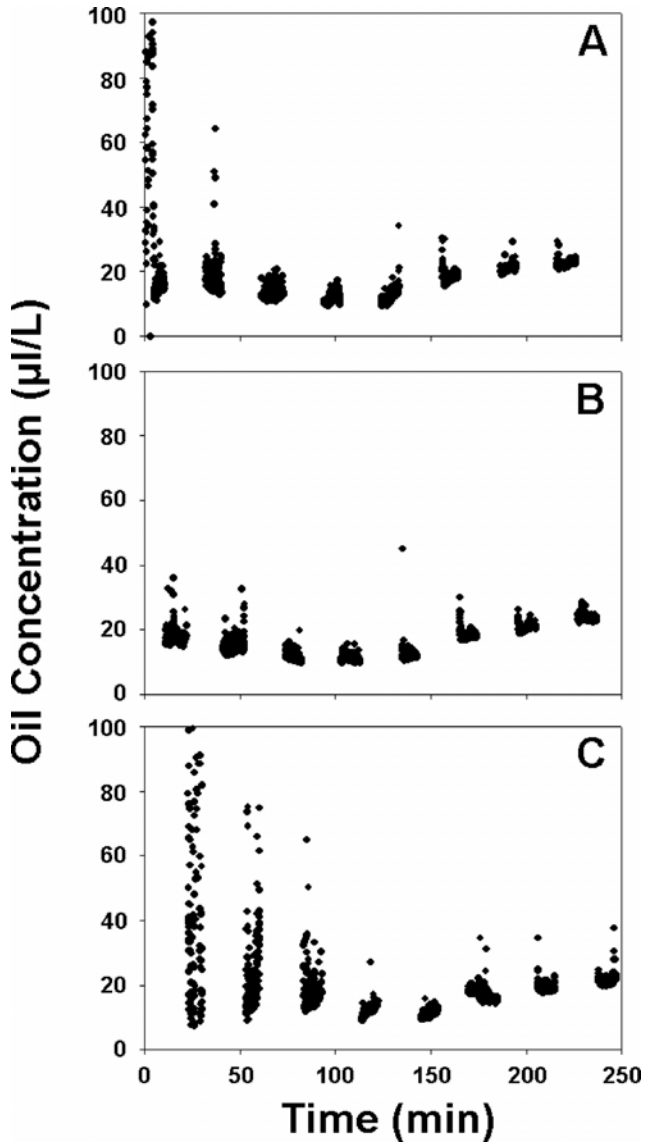


Figure 3. The total dispersed oil concentration measured using LISST-100X: (A) near surface (45 cm), (B) in the middle (80 cm), and (C) near bottom (120 cm).

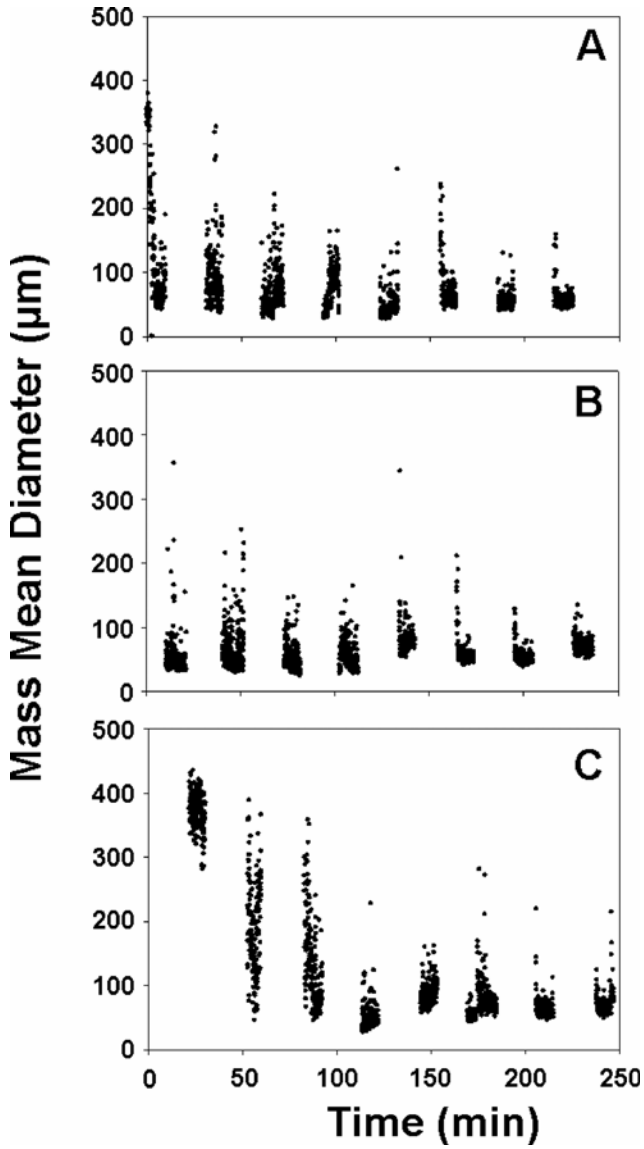


Figure 4. The mass mean diameter of the dispersed oil droplets measured using LISST-100X: (A) near surface (45 cm), (B) in the middle (80 cm), and (C) near bottom (120 cm).

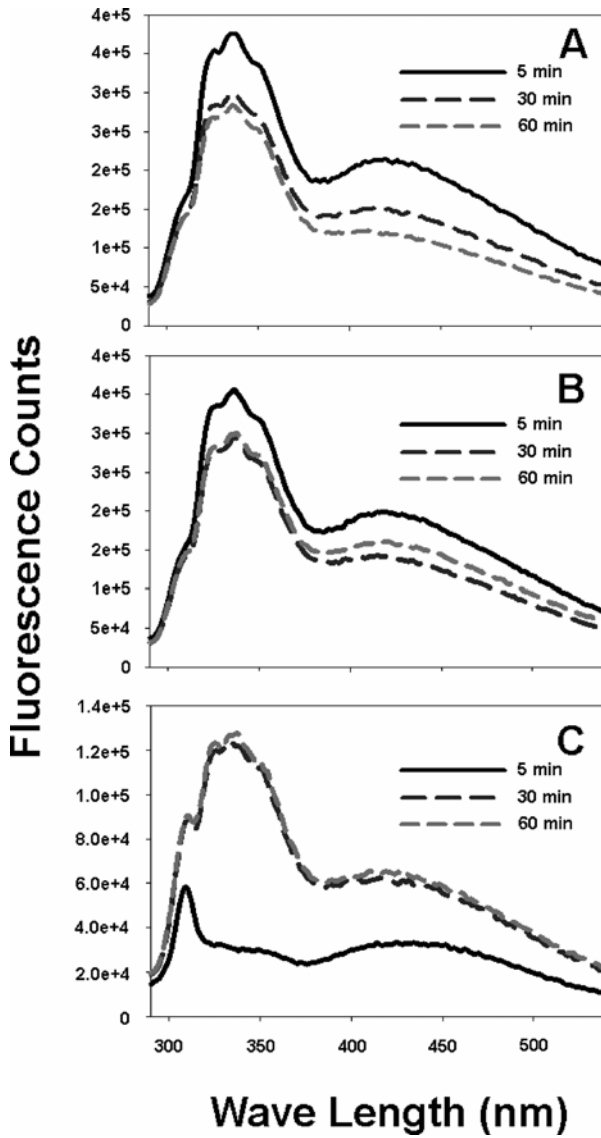


Figure 5. The fluorescence response (UVF) of samples taken from downstream end of the wave tank (L = 20 m from the flap) from three depths: (A) near surface (5 cm), (B) in the middle (75 cm), and (C) near bottom (140 cm).

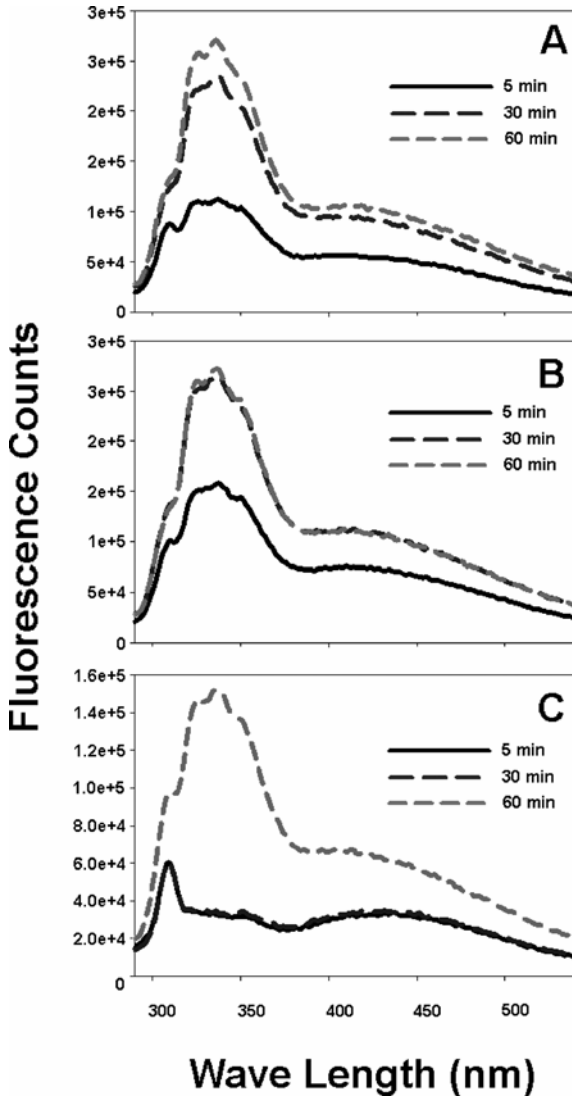


Figure 6. The fluorescence response (UVF) of samples taken from downstream middle of the wave tank ($L = 14$ m from the flap) from three depths: (A) near surface (5 cm), (B) in the middle (75 cm), and (C) near bottom (140 cm).

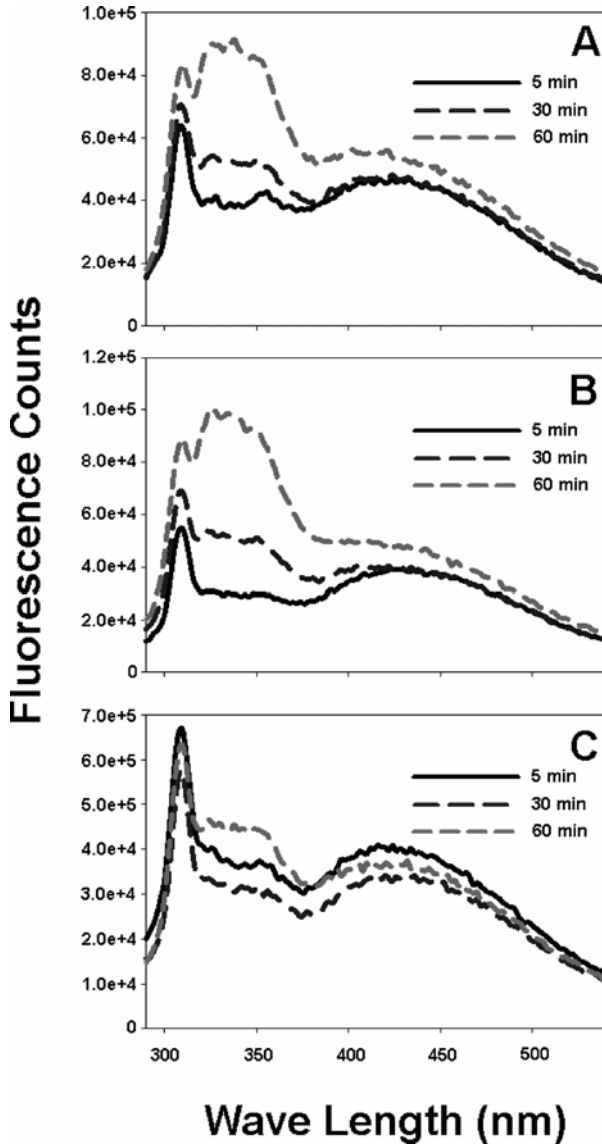


Figure 7. The fluorescence response (UVF) of samples taken from upstream of the wave tank ($L = 8$ m from the flap) from three depths: (A) near surface (5 cm), (B) in the middle (75 cm), and (C) near bottom (140 cm).

wave conditions. Generally the total oil concentrations were low near the bottom for these wave conditions, and the observed dispersed oil droplet sizes were also much smaller in this area of the water column.

Figures 5–7 present the emission spectra of the crude oil dispersed at three different horizontal locations (upstream, near downstream, and further downstream of the oil addition spot), three depths (near surface, middle, and near bottom), and over time (5, 30, and 60 min after wave generation). The initial transport of oil is fast, so that the fluorescence counts were the highest at the surface and middle of the water column at the further downstream location (Figure 5A, B). UVF signals also dramatically increased at near bottom at this location with progress of oil dispersion (Figure 5C).

At near downstream location, UVF signals all increased with the progress of dispersion, suggesting that there was a back flow of the oil mass at the bottom of the wave tank after the initial rapid transport to further downstream (Figure 6).

The back flow of oil mass was more clearly demonstrated by the UVF signals shown in the samples taken from the upstream location (Figure 8A, B). The marked increase of the UVF fluorescence counts near surface and in the middle of the water column indicated that dispersed oil droplets were transported upstream by the under water currents. However, the relatively weak signals at near bottom of the upstream sampling location suggest that the dispersed oil droplets may be moving upwards in the absence of turbulence that was produced by energy dissipation from breaking waves in this upstream area of the wave tank (Figure 7C).

4. Conclusions

The data reported in this paper support the following conclusions: First, oil dispersion effectiveness was correlated with energy dissipation rate; elevated dissipation energy promotes the penetration of oil into the bulk aqueous phase; and the presence of dispersant increased the dispersed oil concentration at the same energy levels. Second, the chemical dispersant significantly reduced the oil droplet sizes, especially at low energy states. Third, re-surfacing of oil occurred at static conditions; and the stability of dispersed oil is significantly increased in the presence of dispersant.

5. Acknowledgements

This research was supported by the Panel of Energy Research and Development (PERD) Canada, U.S. EPA (research contract No. 68-C-00-159), and NOAA/UNH Coastal Response Research Center (Grant Number: NA04NOS4190063 UNH Agreement No.: 06-085). Essential technical and logistical support to this research program was provided by Susan Cobanli, Jennifer Dixon, Xiaowei Ma, Peter Thamer, and Matt Arsenault.

References

- Delvigne, G.A.L. and Sweeney, C.E., 1988, Natural dispersion of oil. *Oil and Chemical Pollution*, **4**(4), 281–310.
- Fingas, M.F., 2000, Use of Surfactants for Environmental Applications. In *Surfactants: Fundamentals and Applications to the Petroleum Industry*, Schramm, L.L., Ed. Cambridge University Press, Cambridge, pp. 461–539.
- Hinds, W.C., *Aerosol Technology: Properties, Behavior, and Measurement of Airborne Particles*, 2nd ed. Wiley, New York, 1999.
- Kepkay, P.E., Bugden, J.B.C., Lee, K., and Stoffyn-Egli, P., 2002, Application of ultraviolet fluorescence spectroscopy to monitor oil-mineral aggregate formation. *Spill Science and Technology Bulletin*, **8**(1), 101–108.
- Lessard, R.R. and Demarco, G., 2000, The significance of oil spill dispersants. *Spill Science and Technology Bulletin*, **6**(1), 59–68.
- NRCNA, *Understanding Oil Spill Dispersants: Efficacy and Effects*. The National Academies Press, Washington, DC, 2005.
- NRC, *National Research Council: Understanding Oil Spill Dispersants: Efficacy and Effects*. National Academies Press: Washington, DC, 2005.
- Shaw, J.M., 2003, A microscopic view of oil slick break-up and emulsion formation in breaking waves. *Spill Science and Technology Bulletin*, **8**(5–6), 491–501.
- Sorial, G.A., Venosa, A.D., Koran, K.M., Holder, E., and King, D.W., 2004a, Oil spill dispersant effectiveness protocol. I: impact of operational variables. *Journal of Environmental Engineering-Asce*, **130**(10), 1073–1084.
- Sorial, G.A., Venosa, A.D., Koran, K.M., Holder, E., and King, D.W., 2004b, Oil spill dispersant effectiveness protocol. II: performance of revised protocol. *Journal of Environmental Engineering-ASCE*, **130**(10), 1085–1093.
- Venosa, A.D., King, D.W., and Sorial, G.A., 2002, The baffled flask test for dispersant effectiveness: a round robin evaluation of reproducibility and repeatability. *Spill Science and Technology Bulletin*, **7**(5–6), 299–308.
- Venosa, A.D., Kaku, V.J., Boufadel, M.C., and Lee, K., 2005, In Measuring energy dissipation rates in a wave tank. *International Oil Spill Conference*, Miami, FL, 2005, American Petroleum Institute, Washington DC, Miami, FL.